

Capon Multiuser Receiver for CDMA Systems With Space-Time Coding

Hongbin Li, *Member, IEEE*, Xuguang Lu, and Georgios B. Giannakis, *Fellow, IEEE*

Abstract—We present in this paper a linear blind multiuser receiver, referred to as the Capon receiver, for code-division multiple-access (CDMA) systems utilizing multiple transmit antennas and space-time (ST) block coding. The Capon receiver is designed by exploiting signal structures imposed by both spreading and ST coding. We highlight the unique ST coding induced structure, which is shown to be critical in establishing several analytical results, including self-interference (i.e., spatially mixed signals of the same user) cancellation, receiver output signal-to-interference-and-noise ratio (SINR), and blind channel estimation of the Capon receiver. To resolve the scalar ambiguity intrinsic to all blind schemes, we propose a semi-blind implementation of the Capon receiver, which capitalizes on periodically inserted pilots and the interference suppression ability of the Capon filters, for (slowly) time-varying channels. Numerical examples are presented to compare the Capon receiver with several other training-assisted and (semi-)blind receivers and to illustrate the performance gain of ST-coded CDMA systems over those without ST coding.

Index Terms—Channel estimation, code division multiple access, interference suppression, multiuser receiver, space-time coding, transmit diversity.

I. INTRODUCTION

FUTURE wireless mobile networks are envisioned to provide capacities and transmission rates by orders of magnitude higher than state-of-the-art systems [1]. Space-time (ST) coding, which has been under intensive study recently, is considered a promising technique to achieve this challenging goal. Relying on multiple transmit antennas, ST coding provides an effective way to exploit spatial and temporal diversity and is capable of producing dramatic increases in transmission rate [2], [3]. A number of ST coding schemes have been proposed so far, including ST-trellis codes [4] and ST-block codes [5], [6]. Whereas ST-trellis coding achieves both the maximum diversity gain and coding advantage, the trellis complexity (and, thus, the decoding complexity) increases exponentially with the transmission rate (see [4, Lemma 3.3.2]). Meanwhile, ST-block coding offers the maximum diversity gain based on linear pro-

cessing at the receiver [5], [6]. Despite a loss in coding advantage, ST-block coding is still attractive, particularly in complexity-sensitive applications, since diversity gain is very effective in reducing the error probability at high signal-to-noise ratio (SNR) [3], [4].

To facilitate coherent decoding of ST codes, the channel state information (CSI) has to be estimated at the receiver either by training or blind methods. As multichannel state information is required for multiantenna systems, channel estimation in ST-coded systems is significantly more difficult than in single-antenna systems [3]. For example, the amount of training data required by training-assisted methods increases proportionally with the number of transmit and receive antennas, causing a substantial decrease of the throughput. To circumvent the difficulty of channel estimation, differential ST coding schemes [7]–[10] can be employed. Similar to the scalar (single-antenna) differential modulation scheme, differential decoding of ST codes incurs approximately a 3-dB penalty in SNR compared with coherent decoding [3].

Interference suppression in multiantenna systems is also more challenging than single-antenna systems [3], [11]. For a system with K users where each is equipped with M transmitting antennas, multiuser interference (MUI) is composed of $(K - 1)M$ interfering signals, rather than $K - 1$ interfering signals in a single-antenna system. Furthermore, multiantenna systems are subject to *self-interference*, which consists of spatially mixed signals of the same user due to simultaneous transmission from multiple transmit antennas.

This paper considers the problem of multiuser receiver design for direct-sequence (DS) code-division multiple-access (CDMA) systems employing multiple transmit antennas and ST-block coding. Specifically, we are interested in extending a linear blind detection technique, which is referred to as the Capon receiver because of its resemblance to the classical Capon spectral estimator [12], to ST-coded CDMA systems. The Capon technique has been successfully utilized in conventional CDMA systems without ST coding (e.g., [13]–[15]) by exploiting the signal structure induced by spreading. However, in order to effectively address the aforementioned difficulties of channel estimation and interference suppression in multi-antenna systems, not only the structure induced by spreading but also that by ST coding should be judiciously exploited in the receiver design for ST-coded CDMA systems. In this paper, we highlight the unique signal structure imposed by ST coding. We show that the inherent signal structure is critical in establishing several analytical results on self-interference cancellation, receiver output signal-to-interference-and-noise ratio (SINR), and blind channel estimation of the Capon receiver. We also

Manuscript received April 24, 2001; revised December 10, 2001. This work was supported by the New Jersey Center for Wireless Telecommunications (NJCWT). The associate editor coordinating the review of this paper and approving it for publication was Dr. Naofal M. W. Al-Dhahir.

H. Li is with the Department of Electrical and Computer Engineering, Stevens Institute of Technology, Hoboken, NJ 07030 USA (e-mail: hli@stevens-tech.edu).

X. Lu was with the Department of Electrical and Computer Engineering, Stevens Institute of Technology, Hoboken, NJ 07030 USA. He is now with Bell Laboratories, Lucent Technologies, Florham Park, NJ 07932 USA.

G. B. Giannakis is with the Department of Electrical and Computer Engineering, University of Minnesota, Minneapolis, MN 55455 USA (e-mail: georgios@ece.umn.edu).

Publisher Item Identifier S 1053-587X(02)03287-7.

discuss how to resolve the scalar ambiguity that exists in all blind schemes by introducing a *semi-blind* implementation for the Capon receiver. We present numerical results to compare the performance of the Capon and several other receivers and to show the performance gain offered by ST coding compared with systems without ST coding.

We focus herein on the downlink (base to mobile) since due to the size/power/cost limitations at the mobile terminal, multiple antennas are more frequently installed at the base station than at the other end. Another consideration is the *asymmetric* nature of future traffic, which requires a higher transmission rate in the downlink than in the uplink (mobile to base) [16]. Transmit diversity is thus recommended in future downlink transmissions [2], [3] in order to break/relieve the bottleneck in that direction. The techniques discussed in the paper, however, have no difficulty in accommodating uplink applications, providing multiple antennas are available at the mobile.

The rest of the paper is organized as follows. In Section II, we introduce the data model and formulate the problem of interest. In Section III, we briefly discuss the linear zero-forcing (ZF) and minimum-mean-squared-error (MMSE) receivers, both explicitly requiring the CSI. The blind Capon receiver is derived in Section IV. The analytical results for the blind Capon receiver are presented in Section V. The semi-blind implementation of the Capon receiver is discussed in Section VI. Section VII contains numerical examples. Finally, the paper is concluded in Section VIII.

Notation: Vectors (matrices) are denoted by boldface lower (upper) case letters; all vectors are column vectors; superscripts $(\cdot)^*$, $(\cdot)^T$, $(\cdot)^H$ denote the complex conjugate, transpose, and conjugate transpose, respectively; \mathbf{I}_M denotes the $M \times M$ identity matrix; $\mathbf{0}$ denotes a zero matrix/vector with all zero entries; $\text{diag}\{\mathbf{B}_1, \dots, \mathbf{B}_M\}$ denotes a block-diagonal matrix with diagonal blocks $\mathbf{B}_1, \dots, \mathbf{B}_M$; $\text{ran}(\cdot)$ denotes the range of a matrix; \mathbf{A}^{-*} denotes $(\mathbf{A}^*)^{-1}$ or, equivalently, $(\mathbf{A}^{-1})^*$; \mathbf{A}^\dagger denotes the Moore–Penrose pseudoinverse [17]; $E\{\cdot\}$ denotes the statistical expectation; $\|\cdot\|$ denotes the matrix/vector Frobenius norm [17]; $\text{tr}\{\cdot\}$ denotes the trace of a matrix; \otimes denotes the Kronecker product [17].

II. SYSTEM MODEL

Consider a synchronous (downlink) K -user CDMA system equipped with M ($M \geq 2$) transmit antennas (TxS) and N ($N \geq 1$) receive antennas (RxS). We assume the Alamouti's ST coding scheme [5], which utilizes $M = 2$ TxS, although other ST-block coding schemes can also be employed. According to the Alamouti's scheme, during the $(2t - 1)$ st (t is an integer) symbol interval, two symbols $b(2t - 1)$ and $b(2t)$ drawn from some constellation are transmitted from Tx1 and Tx2, respectively; during the next symbol interval, $-b^*(2t)$ and $b^*(2t - 1)$ are transmitted from Tx1 and Tx2, respectively.

We assume that the channel is frequency-flat and static (or changes slowly so that standard adaptive schemes can be used to track the fading). Each user is assigned a different spreading code for each Tx. The two spreading codes for one user may be formed from a single spreading code \mathbf{c} as follows: $[\mathbf{c}^T, \mathbf{0}^T]^T$ and $[\mathbf{0}^T, \mathbf{c}^T]^T$, respectively, a scheme recently proposed to UMTS W-CDMA [18], [19] or $[\mathbf{c}^T, \mathbf{c}^T]^T$ and $[\mathbf{c}^T, -\mathbf{c}^T]^T$, respectively,

a scheme adopted in the IS-2000 standard [19], [20]. In this paper, the spreading codes are not restricted to be mutually orthogonal.

The received signal first passes through a chip-matched filter followed by chip-rate sampling. The data vectors collected at Rx n over two consecutive symbol periods is given by [5]

$$\mathbf{x}_n(2t - 1) = \sum_{k=1}^K \sqrt{\rho_k} [h_{1n} \mathbf{c}_{1k} b_k(2t - 1) + h_{2n} \mathbf{c}_{2k} b_k(2t)] + \mathbf{w}_n(2t - 1) \quad (1)$$

$$\mathbf{x}_n(2t) = \sum_{k=1}^K \sqrt{\rho_k} [-h_{1n} \mathbf{c}_{1k} b_k^*(2t) + h_{2n} \mathbf{c}_{2k} b_k^*(2t - 1)] + \mathbf{w}_n(2t) \quad (2)$$

$t = 1, \dots, T; \quad n = 1, \dots, N$

where $\mathbf{x}_n(t) \in \mathbb{C}^{J \times 1}$ consists of data samples within the t th symbol interval at Rx n

ρ_k power of user k ;

h_{mn} channel coefficient from Tx m to Rx n modeled as a complex Gaussian random variable with zero-mean and unit-variance;

\mathbf{c}_{mk} $J \times 1$ spreading code for user k and Tx m ;

$b_k(t)$ t th information symbol for user k drawn from a *unit-energy* constellation;

and $\mathbf{w}_n(t) \in \mathbb{C}^{J \times 1}$ consists of noise/interference samples within the t th symbol interval at Rx n modeled as a zero-mean stationary random vector that is independent of the user symbols. We note that $\mathbf{w}_n(t)$ may be *colored* and *non-Gaussian* due to, e.g., intercell interference (ICI) and narrowband interference in cellular overlay systems [21].

Let $\mathbf{y}_n(t) := [\mathbf{x}_n^T(2t - 1), \mathbf{x}_n^H(2t)]^T$ and $\mathbf{v}_n(t) := [\mathbf{w}_n^T(2t - 1), \mathbf{w}_n^H(2t)]^T$. Then, $\mathbf{y}_n(t)$ is given by

$$\mathbf{y}_n(t) = \sum_{k=1}^K \sqrt{\rho_k} [\mathbf{g}_{nk} b_k(2t - 1) + \bar{\mathbf{g}}_{nk} b_k(2t)] + \mathbf{v}_n(t)$$

where

$$\mathbf{g}_{nk} := [h_{1n} \mathbf{c}_{1k}^T, h_{2n}^* \mathbf{c}_{2k}^T]^T = \mathbf{D}_k \mathbf{h}_n \quad (3)$$

$$\bar{\mathbf{g}}_{nk} := [h_{2n} \mathbf{c}_{2k}^T, -h_{1n}^* \mathbf{c}_{1k}^T]^T = \bar{\mathbf{D}}_k \mathbf{h}_n^* \quad (4)$$

$$\mathbf{D}_k := \begin{bmatrix} \mathbf{c}_{1k} & \mathbf{0} \\ \mathbf{0} & \mathbf{c}_{2k} \end{bmatrix}, \bar{\mathbf{D}}_k := \begin{bmatrix} \mathbf{0} & \mathbf{c}_{2k} \\ -\mathbf{c}_{1k} & \mathbf{0} \end{bmatrix} \quad (5)$$

$$\mathbf{h}_n := [h_{1n}, h_{2n}^*]^T.$$

We next collect the outputs of all receive antennas and define vectors $\mathbf{y}(t) := [\mathbf{y}_1^T(t), \dots, \mathbf{y}_N^T(t)]^T$, $\mathbf{v}(t) := [\mathbf{v}_1^T(t), \dots, \mathbf{v}_N^T(t)]^T$, $\mathbf{h} := [\mathbf{h}_1^T, \dots, \mathbf{h}_N^T]^T$, $\mathbf{g}_k := [\mathbf{g}_{1k}^T, \dots, \mathbf{g}_{Nk}^T]^T = \mathbf{D}_k \mathbf{h}$, and $\bar{\mathbf{g}}_k := [\bar{\mathbf{g}}_{1k}^T, \dots, \bar{\mathbf{g}}_{Nk}^T]^T = \bar{\mathbf{D}}_k \mathbf{h}^*$, where

$$\mathbf{D}_k := \mathbf{I}_N \otimes \mathbf{D}_k, \quad \bar{\mathbf{D}}_k := \mathbf{I}_N \otimes \bar{\mathbf{D}}_k. \quad (6)$$

Assuming the first user is desired, $\mathbf{y}(t)$ can be expressed as

$$\mathbf{y}(t) = \sum_{k=1}^K \sqrt{\rho_k} [\mathbf{g}_k b_k(2t - 1) + \bar{\mathbf{g}}_k b_k(2t)] + \mathbf{v}(t) \quad (7)$$

$$:= \sqrt{\rho_1} [\mathbf{g}_1 b_1(2t - 1) + \bar{\mathbf{g}}_1 b_1(2t)] + \boldsymbol{\nu}(t)$$

where $\boldsymbol{\nu}(t)$ lumps together the MUI and $\mathbf{v}(t)$.

The problem of interest here is to design a linear receiver $\mathbf{F} \in \mathbb{C}^{2JN \times 2}$ that passes with little distortion the desired signal components, i.e., the terms within the square brackets of the last equality of (7), while suppressing the MUI and possibly other sources of interference that are contained in $\mathbf{v}(t)$. The receiver \mathbf{F} can then be applied to the received data $\mathbf{y}(t)$ to yield a soft estimate $\mathbf{z}_1 := \mathbf{F}^H \mathbf{y}(t)$ of $\mathbf{b}_1(t) = [b_1(2t-1), b_1(2t)]^T$.

III. ZERO-FORCING AND MMSE RECEIVERS

When the channel \mathbf{h} is available at the receiver, standard techniques such as the zero-forcing (ZF) and MMSE detection schemes can be used to solve the problem of interest, which are briefly discussed next. Let $\mathcal{D} := [\mathcal{D}_1, \bar{\mathcal{D}}_1, \dots, \mathcal{D}_K, \bar{\mathcal{D}}_K]$, $\mathbf{H} := \text{diag}\{\sqrt{\rho_1}\mathbf{h}, \sqrt{\rho_1}\mathbf{h}^*, \dots, \sqrt{\rho_K}\mathbf{h}, \sqrt{\rho_K}\mathbf{h}^*\} \in \mathbb{C}^{4KN \times 2K}$, $\mathbf{b}_k(t) := [b_k(2t-1), b_k(2t)]^T$, and $\mathbf{b}(t) := [\mathbf{b}_1^T(t), \dots, \mathbf{b}_K^T(t)]^T$. Then, (7) can be more compactly written as

$$\mathbf{y}(t) = \mathcal{D}\mathbf{H}\mathbf{b}(t) + \mathbf{v}(t), \quad t = 1, \dots, T. \quad (8)$$

Supposing that, in addition to the knowledge of \mathbf{h} , the receiver also knows the spreading codes for all users, the ZF receiver $\mathcal{F}_{zf} \in \mathbb{C}^{2JN \times 2K}$ is given by $\mathcal{F}_{zf} = (\mathcal{D}^\dagger)^H \mathbf{H}$, where \mathcal{D} is assumed to have full column rank. It follows that

$$\mathbf{z}(t) := \mathcal{F}_{zf}^H \mathbf{y}(t) = \mathcal{H}\mathbf{b}(t) + \mathbf{H}^H \mathcal{D}^\dagger \mathbf{v}(t) \quad (9)$$

where

$$\begin{aligned} \mathcal{H} &= \mathbf{H}^H \mathbf{H} \\ &= \text{diag}\{\rho_1 \|\mathbf{h}\|^2, \rho_1 \|\mathbf{h}\|^2, \dots, \rho_K \|\mathbf{h}\|^2, \rho_K \|\mathbf{h}\|^2\}. \end{aligned}$$

Since $\|\mathbf{h}\|^2 = \sum_{n=1}^N (|h_{1n}|^2 + |h_{2n}|^2)$, (9) implies that the maximum diversity gain of $2N$ has been achieved. Although the ZF receiver eliminates the intracell MUI, it cannot suppress any unmodeled interference signals contained in $\mathbf{v}(t)$.

It is well known that the MMSE receiver reduces to the ZF receiver when $\text{SNR} = \infty$ and yields a better performance than the latter for finite SNR [22]. The MMSE receiver also maximizes the receiver output SINR among all linear receivers [22] and, thus, is the optimum linear receiver in that sense. To facilitate later usages, we derive the MMSE receiver based on the following expression of $\mathbf{y}(t)$, which is slightly different from (8)

$$\mathbf{y}(t) = \mathbf{G}\mathbf{P}\mathbf{b}(t) + \mathbf{v}(t), \quad t = 1, \dots, T \quad (10)$$

where $\mathbf{P} = \text{diag}\{\sqrt{\rho_1}, \sqrt{\rho_1}, \dots, \sqrt{\rho_K}, \sqrt{\rho_K}\}$, and

$$\mathbf{G} = [\mathbf{G}_1, \dots, \mathbf{G}_K], \quad \mathbf{G}_k = [\mathbf{g}_k, \bar{\mathbf{g}}_k]. \quad (11)$$

The MMSE receiver $\mathcal{F}_M \in \mathbb{C}^{2JN \times 2K}$ is obtained by minimizing the mean-squared error criterion

$$\mathcal{F}_M = \arg \min_{\mathcal{F} \in \mathbb{C}^{2JN \times 2K}} E\{\|\mathbf{b}(t) - \mathcal{F}^H \mathbf{y}(t)\|^2\}. \quad (12)$$

The solution to (12) is given by (see, e.g., [22]) $\mathcal{F}_M = \mathbf{R}_{yy}^{-1} \mathbf{R}_{yb}$, where $\mathbf{R}_{yy} = E\{\mathbf{y}(t)\mathbf{y}^H(t)\}$, $\mathbf{R}_{yb} = E\{\mathbf{y}(t)\mathbf{b}^H(t)\} = \mathbf{G}\mathbf{P}$, and where it is assumed that the elements of $\mathbf{b}(t)$ are independently and identically distributed (i.i.d.) and formed from

some unit-energy constellation. If only the first user is of interest, the MMSE receiver reduces to

$$\mathbf{F}_M = \sqrt{\rho_1} \mathbf{R}_{yy}^{-1} \mathbf{G}_1. \quad (13)$$

IV. BLIND CAPON RECEIVER

Both the ZF and MMSE receivers explicitly require the CSI, which is typically obtained via training. In this section, we present a linear blind receiver, which resembles the classical Capon spectral estimator [12] and is thus referred to as the Capon receiver, for ST-coded systems. The Capon receiver

- 1) requires only the spreading codes and timing of the desired user;
- 2) is able to suppress the overall interference, including MUI, ICI, and narrowband interference;
- 3) facilitates adaptive implementation.

The idea is to design a bank of filters (filterbank), each of which passes one signal component of interest without distortion (unit-gain) while suppressing the overall interference in a nonparametric manner. In particular, we can design $\mathbf{F}_C := [\mathbf{f}_C, \bar{\mathbf{f}}_C] \in \mathbb{C}^{2JN \times 2}$, where each column corresponds to one branch of the filterbank, which minimizes the overall receiver output variance while passing the desired signals with unit-gain

$$\begin{aligned} \mathbf{F}_C &= \arg \min_{\mathbf{F} \in \mathbb{C}^{2JN \times 2}} \text{tr}\{\mathbf{F}^H \mathbf{R}_{yy} \mathbf{F}\}, \quad \text{subject to} \\ &\mathbf{f}^H \mathbf{g}_C = 1 \quad \text{and} \quad \bar{\mathbf{f}}^H \bar{\mathbf{g}}_C = 1 \end{aligned} \quad (14)$$

where $\mathbf{F} = [\mathbf{f}, \bar{\mathbf{f}}]$, \mathbf{g}_C and $\bar{\mathbf{g}}_C$ are estimates (to be determined next) of the true parameters \mathbf{g}_1 and $\bar{\mathbf{g}}_1$, respectively.

Since \mathbf{R}_{yy} is non-negative and $\text{tr}\{\mathbf{F}^H \mathbf{R}_{yy} \mathbf{F}\} = \mathbf{f}^H \mathbf{R}_{yy} \mathbf{f} + \bar{\mathbf{f}}^H \mathbf{R}_{yy} \bar{\mathbf{f}}$, minimizing the trace is equivalent to minimizing the two individual terms separately. Doing so while enforcing the constraints in (14) yields (see, e.g., [23])

$$\begin{aligned} \mathbf{f}_C &= (\mathbf{g}_C^H \mathbf{R}_{yy}^{-1} \mathbf{g}_C)^{-1} \mathbf{R}_{yy}^{-1} \mathbf{g}_C \\ \bar{\mathbf{f}}_C &= (\bar{\mathbf{g}}_C^H \mathbf{R}_{yy}^{-1} \bar{\mathbf{g}}_C)^{-1} \mathbf{R}_{yy}^{-1} \bar{\mathbf{g}}_C \end{aligned} \quad (15)$$

where \mathbf{R}_{yy} is assumed invertible (and thus positive definite). Substituting (15) into the cost function in (14) yields the minimum variance as

$$(\mathbf{g}_C^H \mathbf{R}_{yy}^{-1} \mathbf{g}_C)^{-1} + (\bar{\mathbf{g}}_C^H \mathbf{R}_{yy}^{-1} \bar{\mathbf{g}}_C)^{-1}. \quad (16)$$

It is straightforward to verify that the Capon receiver reduces to the MMSE receiver if we choose $\mathbf{g}_C = (\sqrt{\rho_1} \mathbf{g}_1^H \mathbf{R}_{yy}^{-1} \mathbf{g}_1)^{-1} \mathbf{g}_1$ and $\bar{\mathbf{g}}_C = (\sqrt{\rho_1} \bar{\mathbf{g}}_1^H \mathbf{R}_{yy}^{-1} \bar{\mathbf{g}}_1)^{-1} \bar{\mathbf{g}}_1$. However, the above choice requires knowledge of the CSI. To obtain blind estimates of \mathbf{g}_C and $\bar{\mathbf{g}}_C$, we can maximize (16) with respect to the unknowns so that the signal components at the receiver output are maximized after interference suppression. The maximization, however, appears rather involved due to the nonlinear dependence of (16) on the unknowns. We will instead minimize the sum of the reciprocal of each term of (16), i.e., $\mathbf{g}_C^H \mathbf{R}_{yy}^{-1} \mathbf{g}_C + \bar{\mathbf{g}}_C^H \mathbf{R}_{yy}^{-1} \bar{\mathbf{g}}_C$ or, equivalently

$$\mathbf{g}_C^H \mathbf{R}_{yy}^{-1} \mathbf{g}_C + \bar{\mathbf{g}}_C^T \mathbf{R}_{yy}^{-*} \bar{\mathbf{g}}_C^* \quad (17)$$

where we have used the fact that $\bar{\mathbf{g}}_C^H \mathbf{R}_{yy}^{-1} \bar{\mathbf{g}}_C$ is real-valued. It turns out that minimizing (17) and maximizing (16) are actually equivalent, due to a certain conjugate symmetric structure of \mathbf{g}_C and $\bar{\mathbf{g}}_C$ induced by ST coding; see Lemma 3 in Section V. We next observe the following structure of \mathbf{g}_C and $\bar{\mathbf{g}}_C$: $\mathbf{g}_C = \mathcal{D}_1 \mathbf{h}_C$, and $\bar{\mathbf{g}}_C = \bar{\mathcal{D}}_1 \mathbf{h}_C^*$, where \mathcal{D}_1 and $\bar{\mathcal{D}}_1$ are given by (6), and \mathbf{h}_C denotes the to-be-determined Capon estimate of the true channel parameter \mathbf{h} . Minimizing (17) with respect to \mathbf{h}_C yields

$$\mathbf{h}_C = \arg \min_{\mathbf{h} \in \mathbb{C}^{2N \times 1}} \mathbf{h}^H \underbrace{\left[\mathcal{D}_1^H \mathbf{R}_{yy}^{-1} \mathcal{D}_1 + \bar{\mathcal{D}}_1^H \mathbf{R}_{yy}^{-1} \bar{\mathcal{D}}_1 \right]}_{:=\Omega} \mathbf{h}. \quad (18)$$

The solution to (18), subject to the standard constraint $\|\mathbf{h}_C\| = 1$, is the eigenvector that corresponds to the smallest eigenvalue of Ω . A few remarks are in order.

Remark 1: Note that Ω has a dimension of $2N \times 2N$. Compared with subspace-based blind receivers (e.g., MUSIC [24]), which usually require an eigendecomposition of the $2JN \times 2JN$ covariance matrix \mathbf{R}_{yy} , the Capon receiver is computationally more efficient. The major computation burden of the Capon receiver comes from the calculation of \mathbf{R}_{yy}^{-1} , which can be adaptively and efficiently calculated, resulting in recursive least squares (RLS) like adaptive implementations. Least mean square (LMS) like implementations of the Capon receiver are also possible; see, e.g., [14].

Remark 2: The Capon receiver lumps the interference (intra-cell MUI and other sources of interference) and channel noise in a single *unstructured* term. It is expected that the Capon receiver can deal with colored noise and suppress the overall interference, as has also been confirmed by simulations. On the other hand, subspace methods like MUSIC assume a more restrictive parametric model on the received data and is more sensitive to unknown/unmodeled interference. See Section VII for numerical examples regarding this issue.

V. PERFORMANCE ANALYSIS

The conventional Capon receiver for CDMA systems without ST coding was studied in [13]–[15]. It was shown that the blind Capon channel estimate is consistent (for high SNR) and that the Capon receiver yields an output SINR that is close to that of the optimum linear MMSE receiver [15]. Owing to the use of multiple-antenna transmission and ST coding, the Capon channel estimate and receiver derived in Section IV are notably different from and more complex than those without ST coding, which questions if the above results hold in the current case. As shown in this section, the Alamouti's code (and other ST-block codes obtained from orthogonal design [6] as well) entails a unique signal structure, which can be exploited to establish several analytical results, including the consistency (for high SNR) of the channel estimate and the near-optimality of the receiver output SINR for the Capon receiver derived in Section IV. Furthermore, it renders new insight into the properties of the Capon receiver, such as the immunity to self-interference, which are unique to ST-coded systems. It should be stressed that without the inherent signal structure imposed by ST coding, it would be more difficult to characterize the performance of the Capon receiver, which involves multiple transmit antennas.

To proceed, we make two assumptions that were also used in [15]. First, the information symbols $\{b_k(t)\}$ [cf. (7)] are i.i.d. Second, $\mathbf{v}(t)$ in (7) is an independent *white* process with covariance matrix $\sigma_w^2 \mathbf{I}_{2JN}$. We note that these assumptions are only for analytical tractability and not required by the Capon receiver (see also [25] and [26]). Under these assumptions, the data covariance matrix can be expressed as [cf. (10)]

$$\mathbf{R}_{yy} = \sum_{k=1}^K \rho_k (\mathbf{g}_k \mathbf{g}_k^H + \bar{\mathbf{g}}_k \bar{\mathbf{g}}_k^H) + \sigma_w^2 \mathbf{I}_{2JN}. \quad (19)$$

We expose the inherent structure of the received signal imposed by ST coding through several lemmas.

Lemma 1: Define the generic vectors $\mathbf{g}_k := \mathcal{D}_k \mathbf{h}$ and $\bar{\mathbf{g}}_k := \bar{\mathcal{D}}_k \mathbf{h}^*$, where \mathcal{D}_k and $\bar{\mathcal{D}}_k$ are given by (6), and \mathbf{h} is an arbitrary $2N \times 1$ vector. Let $\mathbf{M}_{2J} := \begin{pmatrix} \mathbf{0} & \mathbf{I}_J \\ -\mathbf{I}_J & \mathbf{0} \end{pmatrix}$. Then, \mathbf{g}_k and $\bar{\mathbf{g}}_k$ satisfy the following conjugate symmetric properties:

$$(\mathbf{I}_N \otimes \mathbf{M}_{2J})^H \bar{\mathbf{g}}_k = \mathbf{g}_k^* \quad (20)$$

$$(\mathbf{I}_N \otimes \mathbf{M}_{2J})^H \mathbf{g}_k = -\bar{\mathbf{g}}_k^*. \quad (21)$$

Proof: See Appendix A. \blacksquare

Lemma 2: Suppose \mathbf{R}_{yy} has a form as in (19). Then, we have

$$(\mathbf{I}_N \otimes \mathbf{M}_{2J})^H \mathbf{R}_{yy}^{-1} (\mathbf{I}_N \otimes \mathbf{M}_{2J}) = \mathbf{R}_{yy}^{-*}. \quad (22)$$

Proof: See Appendix A. \blacksquare

An immediate result following from Lemmas 1 and 2 is that the expression of Ω in (18) can be simplified. To see this, we rewrite the second term of Ω as follows: $\bar{\mathcal{D}}_1^H \mathbf{R}_{yy}^{-1} \bar{\mathcal{D}}_1 = \mathcal{D}_1^H (\mathbf{I}_N \otimes \mathbf{M}_{2J})^H \mathbf{R}_{yy}^{-*} (\mathbf{I}_N \otimes \mathbf{M}_{2J}) \mathcal{D}_1 = \mathcal{D}_1^H [(\mathbf{I}_N \otimes \mathbf{M}_{2J})^H \mathbf{R}_{yy}^{-1} (\mathbf{I}_N \otimes \mathbf{M}_{2J})]^* \mathcal{D}_1 = \mathcal{D}_1^H \mathbf{R}_{yy}^{-1} \mathcal{D}_1$, where the first equality is due to $\bar{\mathcal{D}}_1 = (\mathbf{I}_N \otimes \mathbf{M}_{2J}) \mathcal{D}_1$ [cf. (42)], the second one is due to $\mathbf{I}_N \otimes \mathbf{M}_{2J}$ being real-valued, and Lemma 2 is used in the last equality. It follows that

$$\Omega = 2\mathcal{D}_1^H \mathbf{R}_{yy}^{-1} \mathcal{D}_1. \quad (23)$$

Remark 3: If \mathbf{R}_{yy} is replaced by some estimate (as \mathbf{R}_{yy} is typically unknown in reality) such as the sample covariance matrix

$$\hat{\mathbf{R}}_{yy} = \frac{1}{T} \sum_{t=1}^T \mathbf{y}(t) \mathbf{y}^H(t) \quad (24)$$

then (23) is, in general, not true. In that case, it is preferable to use (18) to estimate Ω since including the second term of Ω in (18) provides additional averaging and can yield better performance than otherwise. In what follows, we will mainly use (23) for analysis and (18) for implementation.

With the above observations in mind, we now proceed to look at two aspects of the Capon receiver, viz. its interference suppression ability and the accuracy of the Capon channel estimate.

A. Self-Interference Cancellation and Output SINR

In addition to MUI, ST-coded CDMA systems are also subject to *self-interference*, i.e., spatially mixed signals of the same user. Unless properly dealt with, self-interference can be devastating (similarly to the effect of intersymbol interference in

dispersive channels). Our first result states that the Capon receiver is by design immune to self-interference.

Theorem 1: For any choices of spreading codes, the Capon receiver $\mathbf{F}_C = [\mathbf{f}_C, \bar{\mathbf{f}}_C]$ given in (15) satisfies the following properties:

$$\mathbf{F}_C^H [\mathbf{g}_C, \bar{\mathbf{g}}_C] = \mathbf{I}_2 \quad (25)$$

$$\bar{\mathbf{f}}_C^H \mathbf{f}_C = 0. \quad (26)$$

Proof: To show (25), it suffices to show that $\mathbf{g}_C^H \mathbf{R}_{yy}^{-1} \bar{\mathbf{g}}_C = 0$. According to Lemmas 1 and 2, we can write

$$\begin{aligned} & \mathbf{g}_C^H \mathbf{R}_{yy}^{-1} \bar{\mathbf{g}}_C \\ &= \bar{\mathbf{g}}_C^T (\mathbf{I}_N \otimes \mathbf{M}_{2J}) \mathbf{R}_{yy}^{-1} \bar{\mathbf{g}}_C \\ &= \bar{\mathbf{g}}_C^T (\mathbf{I}_N \otimes \mathbf{M}_{2J}) (\mathbf{I}_N \otimes \mathbf{M}_{2J})^H \mathbf{R}_{yy}^{-*} (\mathbf{I}_N \otimes \mathbf{M}_{2J}) \bar{\mathbf{g}}_C \\ &= \bar{\mathbf{g}}_C^T \mathbf{R}_{yy}^{-*} (\mathbf{I}_N \otimes \mathbf{M}_{2J}) \bar{\mathbf{g}}_C = -\bar{\mathbf{g}}_C^T \mathbf{R}_{yy}^{-*} \bar{\mathbf{g}}_C^* \\ &= -(\mathbf{g}_C^H \mathbf{R}_{yy}^{-1} \bar{\mathbf{g}}_C)^T = 0 \end{aligned}$$

which, along with the constraint in (14), indicates (25). To show (26), it suffices to show that $\mathbf{g}_C^H \mathbf{R}_{yy}^{-2} \bar{\mathbf{g}}_C = 0$. The proof proceeds similarly. Specifically, we have

$$\begin{aligned} & \mathbf{g}_C^H \mathbf{R}_{yy}^{-2} \bar{\mathbf{g}}_C \\ &= \bar{\mathbf{g}}_C^T (\mathbf{I}_N \otimes \mathbf{M}_{2J}) [(\mathbf{I}_N \otimes \mathbf{M}_{2J})^H \mathbf{R}_{yy}^{-*} (\mathbf{I}_N \otimes \mathbf{M}_{2J})] \\ & \quad \times [(\mathbf{I}_N \otimes \mathbf{M}_{2J})^H \mathbf{R}_{yy}^{-*} (\mathbf{I}_N \otimes \mathbf{M}_{2J})] \bar{\mathbf{g}}_C \\ &= -(\mathbf{g}_C^H \mathbf{R}_{yy}^{-2} \bar{\mathbf{g}}_C)^T = 0 \end{aligned}$$

which concludes the proof. \blacksquare

Hence, the two sub-Capon receivers \mathbf{f}_C and $\bar{\mathbf{f}}_C$ are orthogonal to one another, each passing one of the two signal components of the desired user with unit-gain while canceling mutual interference caused by the other signal component. The cancellation is independent of the spreading codes, which indicates that the cancellation is due to ST coding and not spreading. We may also enforce zero-forcing during filter design by modifying the design constraint of (14) to $\mathbf{F}^H [\mathbf{g}_C, \bar{\mathbf{g}}_C] = \mathbf{I}_2$. We prefer the original constraint since it entails a simpler solution that still cancels the self-interference.

We now examine the receiver output SINR, which shows the overall interference suppression ability of a given receiver. We first break \mathbf{R}_{yy} into three parts: $\mathbf{R}_{yy} := \mathbf{R}_s + \bar{\mathbf{R}}_s + \mathbf{R}_i$, where $\mathbf{R}_s = \rho_1 \mathbf{g}_1 \mathbf{g}_1^H$, $\bar{\mathbf{R}}_s = \rho_1 \bar{\mathbf{g}}_1 \bar{\mathbf{g}}_1^H$, and $\mathbf{R}_i = \sum_{k=2}^K \rho_k \mathbf{G}_k \mathbf{G}_k^H +$

$\sigma_w^2 \mathbf{I}_{2JN}$ denotes the covariance matrix of the MUI plus the noise. Let $\mathbf{F} := [\mathbf{f}, \bar{\mathbf{f}}] \in \mathbb{C}^{2JN \times 2}$ denote a generic receiver. The output SINR can be expressed as

$$\text{SINR} = \frac{\mathbf{f}^H \mathbf{R}_s \mathbf{f} + \bar{\mathbf{f}}^H \bar{\mathbf{R}}_s \bar{\mathbf{f}}}{\mathbf{f}^H (\mathbf{R}_{yy} - \mathbf{R}_s) \mathbf{f} + \bar{\mathbf{f}}^H (\mathbf{R}_{yy} - \bar{\mathbf{R}}_s) \bar{\mathbf{f}}} = \frac{1}{\alpha - 1} \quad (27)$$

$$\alpha = \frac{\mathbf{f}^H \mathbf{R}_{yy} \mathbf{f} + \bar{\mathbf{f}}^H \mathbf{R}_{yy} \bar{\mathbf{f}}}{\mathbf{f}^H \mathbf{R}_s \mathbf{f} + \bar{\mathbf{f}}^H \bar{\mathbf{R}}_s \bar{\mathbf{f}}}. \quad (28)$$

Note that the SINR is a monotonically decreasing function of α .

It would be of interest to compare the Capon receiver with the MMSE receiver since the latter is known to yield the highest output SINR among all linear receivers [15]. For the MMSE receiver $\mathbf{F}_M := [\mathbf{f}_M, \bar{\mathbf{f}}_M]$, we have [see (13)] $\mathbf{f}_M = \sqrt{\rho_1} \mathbf{R}_{yy}^{-1} \mathbf{g}_1$ and $\bar{\mathbf{f}}_M = \sqrt{\rho_1} \mathbf{R}_{yy}^{-1} \bar{\mathbf{g}}_1$. Substituting \mathbf{f}_M and $\bar{\mathbf{f}}_M$ into (28), we obtain $\alpha_M = [\rho_1 (\mathbf{g}_1^H \mathbf{R}_{yy}^{-1} \mathbf{g}_1) + \rho_1 (\bar{\mathbf{g}}_1^H \mathbf{R}_{yy}^{-1} \bar{\mathbf{g}}_1)] / [\rho_1^2 (\mathbf{g}_1^H \mathbf{R}_{yy}^{-1} \mathbf{g}_1)^2 + \rho_1^2 (\bar{\mathbf{g}}_1^H \mathbf{R}_{yy}^{-1} \bar{\mathbf{g}}_1)^2]$. The expression for α_M is somewhat involved and prevents much insight into the behavior of the MMSE receiver. It turns out that α_M can be simplified by exploiting again the inherent signal structure induced by ST coding or, specifically, the following observation.

Lemma 3: The generic vectors \mathbf{g}_k and $\bar{\mathbf{g}}_k$ defined in Lemma 1 satisfy

$$\bar{\mathbf{g}}_k^H \mathbf{R}_{yy}^{-1} \bar{\mathbf{g}}_k = \mathbf{g}_k^H \mathbf{R}_{yy}^{-1} \mathbf{g}_k. \quad (29)$$

Proof: By Lemmas 1 and 2, $\bar{\mathbf{g}}_k^H \mathbf{R}_{yy}^{-1} \bar{\mathbf{g}}_k = (\mathbf{g}_k^*)^H (\mathbf{I}_N \otimes \mathbf{M}_{2J})^H \mathbf{R}_{yy}^{-1} (\mathbf{I}_N \otimes \mathbf{M}_{2J}) \mathbf{g}_k^* = (\mathbf{g}_k^*)^H \mathbf{R}_{yy}^{-*} \mathbf{g}_k^* = (\mathbf{g}_k^H \mathbf{R}_{yy}^{-1} \mathbf{g}_k)^* = \mathbf{g}_k^H \mathbf{R}_{yy}^{-1} \mathbf{g}_k$, where the last equality is because $\mathbf{g}_k^H \mathbf{R}_{yy}^{-1} \mathbf{g}_k$ is real valued. \blacksquare

Using the above result, one can easily see that α_M reduces to

$$\alpha_M = (\rho_1 \mathbf{g}_1^H \mathbf{R}_{yy}^{-1} \mathbf{g}_1)^{-1}. \quad (30)$$

Consider next the Capon receiver $\mathbf{f}_C := [\mathbf{f}_C, \bar{\mathbf{f}}_C]$, where \mathbf{f}_C and $\bar{\mathbf{f}}_C$ are given by (15). Substituting \mathbf{f}_C and $\bar{\mathbf{f}}_C$ into (28), we have (31), shown at the bottom of the page, where the second equality of α_C is again due to (29).

To facilitate a comparison of the MMSE and Capon output SINR, we employ the following eigendecomposition $\mathcal{D}_1^H \mathbf{R}_{yy}^{-1} \mathcal{D}_1 = \sum_{l=1}^{2N} \mu_l \mathbf{u}_l \mathbf{u}_l^H$, where $\mu_1 \geq \dots \geq \mu_{2N}$ denote the eigenvalues, and the associated eigenvectors are $\mathbf{u}_l, l = 1, \dots, 2N$, respectively. Thus, we have $\mathbf{g}_1^H \mathbf{R}_{yy}^{-1} \mathbf{g}_1 = \sum_{l=1}^{2N} \mu_l |\mathbf{h}^H \mathbf{u}_l|^2$. It follows that (30) can be expressed as

$$\alpha_M = \left(\rho_1 \sum_{l=1}^{2N} \mu_l |\mathbf{h}^H \mathbf{u}_l|^2 \right)^{-1}. \quad (32)$$

$$\begin{aligned} \alpha_C &= \frac{(\mathbf{g}_C^H \mathbf{R}_{yy}^{-1} \mathbf{g}_C)^{-1} + (\bar{\mathbf{g}}_C^H \mathbf{R}_{yy}^{-1} \bar{\mathbf{g}}_C)^{-1}}{\rho_1 (\mathbf{g}_C^H \mathbf{R}_{yy}^{-1} \mathbf{g}_C)^{-2} |\mathbf{g}_C^H \mathbf{R}_{yy}^{-1} \mathbf{g}_1|^2 + \rho_1 (\bar{\mathbf{g}}_C^H \mathbf{R}_{yy}^{-1} \bar{\mathbf{g}}_C)^{-2} |\bar{\mathbf{g}}_C^H \mathbf{R}_{yy}^{-1} \bar{\mathbf{g}}_1|^2} \\ &= \frac{\mathbf{g}_C^H \mathbf{R}_{yy}^{-1} \mathbf{g}_C}{\rho_1 |\mathbf{g}_C^H \mathbf{R}_{yy}^{-1} \mathbf{g}_1|^2} \end{aligned} \quad (31)$$

For the Capon α_C , we first note that [cf. (18) and (23)] $\mathbf{h}_C = \mathbf{u}_{2N}$ and $\mathbf{g}_C^H \mathbf{R}_{yy}^{-1} \mathbf{g}_C = \mu_{2N}$. Furthermore, we have $\mathbf{g}_C^H \mathbf{R}_{yy}^{-1} \mathbf{g}_1 = \mathbf{u}_{2N}^H (\sum_{l=1}^{2N} \mu_l \mathbf{u}_l \mathbf{u}_l^H) \mathbf{h} = \mu_{2N} \mathbf{u}_{2N}^H \mathbf{h}$. It follows that

$$\alpha_C = \left(\rho_1 \mu_{2N} |\mathbf{u}_{2N}^H \mathbf{h}|^2 \right)^{-1}. \quad (33)$$

Comparing (32) and (33) indicates that $\alpha_M \leq \alpha_C$, and therefore, $\text{SINR}_M \geq \text{SINR}_C$. It can be shown that the inequality becomes an equality if orthogonal spreading codes are used. Even though SINR_C is, in general, smaller than SINR_M for nonorthogonal spreading codes, the difference in SINR decreases and tends to a small constant as the SNR increases, as summarized in the next result.

Theorem 2: The output SINR for the Capon and MMSE receivers are related by the equation shown at the bottom of the page, where \mathcal{D}_1 is defined by (6), \mathbf{E}_s , \mathbf{E}_n , and Σ_s are defined by the eigendecomposition of \mathbf{R}_{yy}

$$\mathbf{R}_{yy} = \mathbf{E}_s \Sigma_s \mathbf{E}_s^H + \sigma_w^2 \mathbf{E}_n \mathbf{E}_n^H. \quad (34)$$

Proof: The proof proceeds by a first-order (in σ_w^2) perturbation analysis of α_M and α_C as given by (32) and (33), respectively, similar to the proof of Proposition 4 of [15]. See [15] for details. ■

Hence, like the conventional Capon receiver [15], the Capon receiver for ST-coded CDMA systems also achieves an output SINR close to that of the optimum linear MMSE receiver. It should be noted that without the ST coding induced signal structure, which renders the simplified expressions of α_C in (31) and α_M in (30), the relation between the MMSE and Capon receivers would be more elusive to determine.

B. Channel Estimation

The matrix Ω in (23) is, in general, full rank with distinct eigenvalues with probability one, which implies that the Capon channel estimate is unique (up to a scalar). However, how accurate this estimate is remains a question. The following result indicates that in the absence of noise, the Capon channel estimate is not only unique but also exact (up to a scalar).

Theorem 3: The channel estimate \mathbf{h}_C in (18) is unique and exact (up to a scalar) at $\text{SNR} = \infty$ 1) if the spreading codes \mathbf{c}_{11} and \mathbf{c}_{21} for the first user are linearly independent of each other as well as linearly independent of the spreading codes of all other users and 2) if $\mathbf{h}_n = [h_{1n}, h_{2n}^*]^T \neq \mathbf{0}$ for some n .

Proof: See Appendix B. ■

Note that the above conditions are usually met in a real system. Our next result establishes the consistency (for high SNR) of the Capon channel estimate.

Theorem 4: Under the conditions stated in Theorem 3 and for small σ_w^2 , \mathbf{h}_C in (18) satisfies

$$\mathbf{h}_C = \mathbf{h}/\|\mathbf{h}\| + \epsilon \quad (35)$$

where $\epsilon \approx -(\sigma_w^2/\|\mathbf{h}\|)(\mathcal{D}_1^H \mathbf{E}_n \mathbf{E}_n^H \mathcal{D}_1)^\dagger \mathcal{D}_1^H \mathbf{E}_s \Sigma_s^{-1} \mathbf{E}_s^H \mathcal{D}_1 \mathbf{h}$ and where \mathcal{D}_1 , \mathbf{E}_n and Σ_s are defined as in Theorem 2.

Proof: The proof proceeds by a first-order (in σ_w^2) analysis of the eigenvalues and eigenvectors of Ω using the simplified form (23). See [15, Prop. 3] for a similar proof. ■

Theorem 4 indicates that at high SNR, the estimation error is proportional to the noise variance σ_w^2 . Hence, the Capon channel estimate is consistent (in SNR), which is similar to the conventional Capon receiver in [15]. It should be stressed again that Theorem 4 is valid because of the signal structure imposed by ST coding. Without such, the SNR consistency of the Capon channel estimate would be more difficult, if not impossible, to establish.

VI. SEMIBLIND IMPLEMENTATION

One problem inherent to all blind estimators, including the Capon receiver, is the scalar ambiguity associated with the channel estimates [27]. The scalar ambiguity has to be resolved to prevent phase rotation in the detected symbols. Another inherent problem for all blind schemes relying on an estimate of \mathbf{R}_{yy} is the relative slow convergence. When the sample covariance matrix $\hat{\mathbf{R}}_{yy}$ in (24) is used, we need at least $T = 2JN$ [cf. (1)–(2)] blocks of data so that $\hat{\mathbf{R}}_{yy}$ is invertible. Considerably more data samples may be required in order to obtain a reliable estimate $\hat{\mathbf{R}}_{yy}$ (see Fig. 4 for a numerical example on this aspect).

In order to resolve the scalar ambiguity, improve data efficiency, and facilitate tracking of time-varying channels, we will introduce a semi-blind implementation of the Capon receiver that builds on training symbols (pilots). Pilots are routinely used in real systems for synchronization and/or channel estimation. Semi-blind schemes usually yield reduced training overhead and improved performance over methods relying completely on training, particularly in time-varying channels (also see the numerical examples in Section VII). The proposed semi-blind Capon receiver consists of the following steps.

$\text{SINR}_C/\text{SINR}_M \rightarrow (1 + \eta)^{-1}$, as $\text{SNR} \rightarrow \infty$, where

$$\eta = \frac{\left\| \left[(\mathcal{D}_1^H \mathbf{E}_n \mathbf{E}_n^H \mathcal{D}_1)^\dagger \right]^{1/2} \mathcal{D}_1^H \mathbf{E}_s (\Sigma_s - \sigma_w^2 \mathbf{I}_{2K})^{-1} \mathbf{E}_s \mathcal{D}_1 \mathbf{h} \right\|^2}{\left\| (\Sigma_s - \sigma_w^2 \mathbf{I}_{2K})^{-1} \mathbf{E}_s^H \mathcal{D}_1 \mathbf{h} \right\|^2}$$

- 1) Obtain an initial channel estimate $\widehat{\sqrt{\rho_1}}\mathbf{h}^{(0)}$ via training (e.g., least-squares fitting), estimate the covariance matrix as

$$\widehat{\mathbf{R}}_{yy}^{(0)} = \widehat{\mathbf{g}}_1^{(0)}\widehat{\mathbf{g}}_1^{(0)H} + \widehat{\mathbf{g}}_1^{(0)}\widehat{\mathbf{g}}_1^{(0)H} + \widehat{\sigma}_w^2\mathbf{I}_{2JN} \quad (36)$$

and compute the inverse $(\widehat{\mathbf{R}}_{yy}^{(0)})^{-1}$. Here, $\widehat{\mathbf{g}}_1^{(0)} = \mathcal{D}_1\widehat{\sqrt{\rho_1}}\mathbf{h}^{(0)}$, $\widehat{\mathbf{g}}_1^{(0)} = \widehat{\mathcal{D}}_1(\widehat{\sqrt{\rho_1}}\mathbf{h}^{(0)})^*$, and $\widehat{\sigma}_w^2$ is an initial estimate of the noise variance, which is obtained as, e.g., the averaged power of the received data less the desired signal components. That is, $\widehat{\sigma}_w^2 = (2JNT_{\text{tr}})^{-1} \sum_{t=1}^{T_{\text{tr}}} \|\mathbf{y}(t) - [\widehat{\mathbf{g}}_1^{(0)}, \widehat{\mathbf{g}}_1^{(0)}]\mathbf{b}_1(t)\|^2$, where T_{tr} denotes the number of training blocks. Although (36) is a rather rough estimate of the covariance matrix, it works well enough to get the Capon receiver started. If the spreading codes of other users are known at the receiver, they can be exploited to yield a better initial covariance matrix estimate by enforcing the structure in (19).

- 2) Compute $(\widehat{\mathbf{R}}_{yy}^{(t)})^{-1}$ iteratively each time when a new data block $\mathbf{y}(t)$ becomes available. We can use the standard iteration with forgetting factor $\kappa \in [0, 1]$ [22]

$$\begin{aligned} \widehat{\mathbf{R}}_{yy}^{(t)} &= \kappa\widehat{\mathbf{R}}_{yy}^{(t-1)} + (1-\kappa)\mathbf{y}(t)\mathbf{y}^H(t), \\ (\widehat{\mathbf{R}}_{yy}^{(t)})^{-1} &= \frac{1}{\kappa} (\widehat{\mathbf{R}}_{yy}^{(t-1)})^{-1} \\ &\quad - \frac{1-\kappa}{\kappa^2} \frac{(\widehat{\mathbf{R}}_{yy}^{(t-1)})^{-1} \mathbf{y}(t)\mathbf{y}^H(t) (\widehat{\mathbf{R}}_{yy}^{(t-1)})^{-1}}{1 + (1-\kappa)\mathbf{y}^H(t) (\widehat{\mathbf{R}}_{yy}^{(t-1)})^{-1} \mathbf{y}(t)}. \end{aligned}$$

Alternatively, we can use a sliding window of length L

$$\widehat{\mathbf{R}}_{yy}^{(t)} = \widehat{\mathbf{R}}_{yy}^{(t-1)} + L^{-1}[\mathbf{y}(t)\mathbf{y}^H(t) - \mathbf{y}(t-L)\mathbf{y}^H(t-L)]. \quad (37)$$

$(\widehat{\mathbf{R}}_{yy}^{(t)})^{-1}$ in this case can be recursively computed as (by applying the matrix inversion lemma twice)

$$\begin{aligned} (\widehat{\mathbf{R}}_{yy}^{(t)})^{-1} &= (\widehat{\mathbf{Q}}_{yy}^{(t)})^{-1} \\ &\quad + \frac{(\widehat{\mathbf{Q}}_{yy}^{(t)})^{-1} \mathbf{y}(t-L)\mathbf{y}^H(t-L) (\widehat{\mathbf{Q}}_{yy}^{(t)})^{-1}}{L - \mathbf{y}^H(t-L) (\widehat{\mathbf{Q}}_{yy}^{(t)})^{-1} \mathbf{y}(t-L)} \end{aligned} \quad (38)$$

$$\begin{aligned} (\widehat{\mathbf{Q}}_{yy}^{(t)})^{-1} &= (\widehat{\mathbf{R}}_{yy}^{(t-1)})^{-1} \\ &\quad - \frac{(\widehat{\mathbf{R}}_{yy}^{(t-1)})^{-1} \mathbf{y}(t)\mathbf{y}^H(t) (\widehat{\mathbf{R}}_{yy}^{(t-1)})^{-1}}{L + \mathbf{y}^H(t) (\widehat{\mathbf{R}}_{yy}^{(t-1)})^{-1} \mathbf{y}(t)}. \end{aligned} \quad (39)$$

- 3) Update the Capon blind channel estimate $\widehat{\mathbf{h}}_C^{(t)}$ based on $(\widehat{\mathbf{R}}_{yy}^{(t)})^{-1}$ and (18), and compute the Capon receiver $\widehat{\mathbf{f}}_C^{(t)}$ and $\widehat{\mathbf{f}}_C^{(t)}$ by (15). ($\widehat{\mathbf{h}}_C^{(t)}$, $\widehat{\mathbf{f}}_C^{(t)}$, and $\widehat{\mathbf{f}}_C^{(t)}$ to signify that these quantities are based on the estimated covariance matrix $\widehat{\mathbf{R}}_{yy}^{(t)}$.) The Capon channel estimate and receiver do not need to be computed for every t ; they can be updated periodically for every T_C blocks of data

determined by a tradeoff between complexity and channel fading rate.

- 4) Resolve the scalar ambiguity. Assuming the availability of pilots, the idea is to estimate the ambiguity factor using the prefiltered data, viz., data filtered by $\widehat{\mathbf{F}}_C^{(t)} = [\widehat{\mathbf{f}}_C^{(t)}, \widehat{\mathbf{f}}_C^{(t)}]$, rather than the raw data. This is because the Capon filter cancels most of the interference and, thus, the prefiltered data is “cleaner” than the raw data for estimating the ambiguity factor. Specifically, suppose pilots are inserted at $t = t_1, \dots, t_{T_P}$ within a cycle of T_C blocks. We assume that the channel remains (approximately) unchanged within T_C blocks, and thus, we drop the time index (t) of all estimated quantities. Ignoring the estimation error, we may write

$$\mathbf{h} = \alpha\widehat{\mathbf{h}}_C, \quad \mathbf{G}_1 = [\alpha\widehat{\mathbf{g}}_C, \quad \alpha^*\widehat{\mathbf{g}}_C]$$

where α is the unknown scalar, \mathbf{G}_1 is given by (11), $\widehat{\mathbf{g}}_C = \mathcal{D}_1\widehat{\mathbf{h}}_C$, and $\widehat{\mathbf{g}}_C = \widehat{\mathcal{D}}_1\widehat{\mathbf{h}}_C^*$. Let $\mathbf{z}_1(t)$ denote the prefiltered data, i.e., $\mathbf{z}_1(t) = \widehat{\mathbf{F}}_C^H \mathbf{y}(t) := [z_1(2t-1), z_1(2t)]^T$. We know from Theorem 1 that $\widehat{\mathbf{F}}_C^H \mathbf{G}_1 = \begin{pmatrix} \alpha & 0 \\ 0 & \alpha^* \end{pmatrix}$. Hence [cf. (7)]

$$\begin{aligned} \mathbf{z}_1(t_i) &= \sqrt{\rho_1}[\alpha b_1(2t_i-1), \quad \alpha^* b_1^*(2t_i)]^T + \widehat{\mathbf{F}}_C^H \boldsymbol{\nu}(t_i) \\ &\quad i = 1, \dots, T_P. \end{aligned} \quad (40)$$

Let $\mathbf{z}_1(t_i) = [z_1(2t_i-1), z_1^*(2t_i)]^T$, $\mathbf{b}(t_i) = [b(2t_i-1), b^*(2t_i)]^T$ and $\boldsymbol{\xi}(t_i)$ be a 2×1 vector formed from the first element and the complex conjugate of the second element of $\widehat{\mathbf{F}}_C^H \boldsymbol{\nu}(t_i)$. It follows from (40) that

$$\mathbf{z}_1(t_i) = \sqrt{\rho_1}\alpha\mathbf{b}(t_i) + \boldsymbol{\xi}(t_i), \quad i = 1, \dots, T_P. \quad (41)$$

The least-squares estimate of $\sqrt{\rho_1}\alpha$ from (41) is given by

$$\widehat{\sqrt{\rho_1}}\alpha = \frac{1}{T_P} \sum_{i=1}^{T_P} \mathbf{b}^H(t_i)\mathbf{z}_1(t_i)/\|\mathbf{b}(t_i)\|^2.$$

Next, compensate for the ambiguity

$$\widehat{\mathbf{g}}_C' = \widehat{\sqrt{\rho_1}}\alpha\widehat{\mathbf{g}}_C, \quad \widehat{\mathbf{g}}_C' = (\widehat{\sqrt{\rho_1}}\alpha)^*\widehat{\mathbf{g}}_C$$

and use $\widehat{\mathbf{g}}_C'$, $\widehat{\mathbf{g}}_C'$ and (15) to redetermine the Capon receiver $\widehat{\mathbf{f}}_C^{(t)'}$ and $\widehat{\mathbf{f}}_C^{(t)'}$.

- 5) Use $\widehat{\mathbf{f}}_C^{(t)'}$ and $\widehat{\mathbf{f}}_C^{(t)'}$ for detection. For BPSK, for example, the decision reduces to

$$\text{sign} \left\{ \Re \left(\left[\widehat{\mathbf{f}}_C^{(t)'}, \widehat{\mathbf{f}}_C^{(t)'} \right]^H \mathbf{y}(t) \right) \right\}.$$

VII. NUMERICAL RESULTS

We consider a ten-user CDMA system that is equipped with $M = 2$ Txs and employs the Alamouti's ST coding scheme with a BPSK constellation. Random spreading codes of length $J = 32$ and unit energy are used for spreading. The receiver is equipped with either $N = 1$ or $N = 2$ Rxes. The simulated

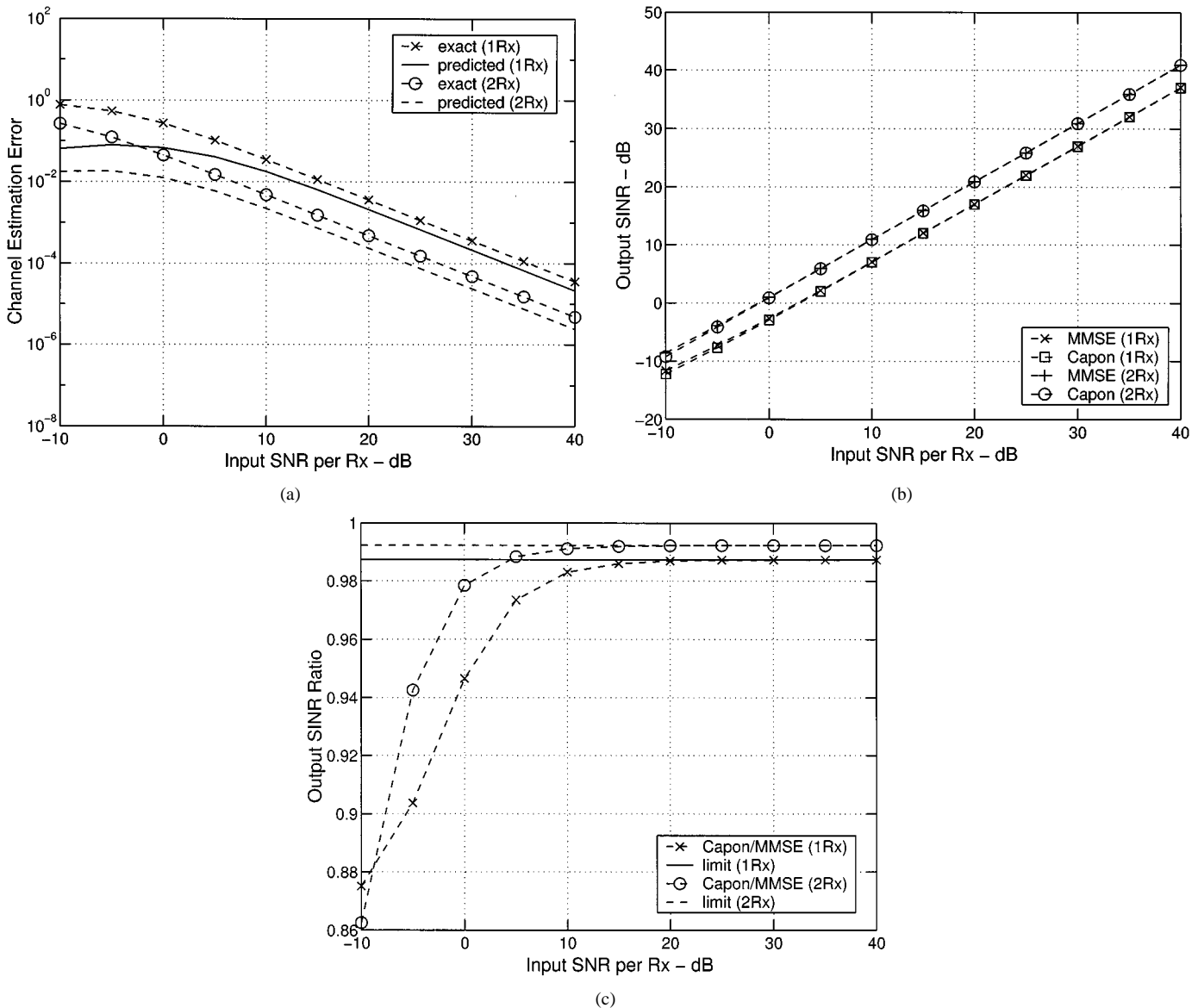


Fig. 1. Performance of the MMSE and blind Capon receivers versus the input SNR per Rx when $J = 32$, $K = 10$ and $\text{NFR} = 10$ dB. (a) Exact and predicted channel estimation error of Capon. (b) Output SINR. (c) Ratio of the output SINR.

channel coefficients are randomly generated, following a complex Gaussian distribution with zero-mean and unit-variance.

We first verify the analytical results obtained in Section V when the additive noise $\mathbf{v}(n)$ [see (7)] is white Gaussian. Assuming that the first user is desired, we simulate a near-far scenario where the power of the nine interfering users is 10 dB larger than that of the first one, that is, the near-far ratio (NFR) is 10 dB. Fig. 1 depicts the performance of the Capon and MMSE receivers when the true covariance matrix \mathbf{R}_{yy} is used for both the Capon and MMSE receivers. In this example, we ignore the inherent ambiguity of the Capon channel estimate \mathbf{h}_C , which is scaled such that the first element of \mathbf{h}_C and that of the true channel vector \mathbf{h} are identical. Fig. 1(a) shows the exact estimation error of the Capon channel estimator (18) and that predicted by Theorem 4. To make the two cases of $N = 1$ and $N = 2$ comparable, the estimation error shown in Fig. 1(a) is $\|\epsilon\|$ [see (35)] normalized by the number of unknown channel coefficients. We see that the channel estimation error decrease as

the SNR increases. We also see that the prediction made by Theorem 4 is quite accurate when the SNR is high. We further note that the channel estimation accuracy improves when a second antenna is included. Fig. 1(b) depicts the output SINR for both the Capon and MMSE receivers as a function of the input SNR per Rx. It is seen that the output SINR of the Capon receiver is very close to that of the MMSE receiver. Improved performance is obtained for both receivers when $N = 2$. Fig. 1(c) shows the ratio of the output SINR of the Capon receiver to that of the MMSE receiver and the limit of the ratio predicted by Theorem 2. The predicted limit of the ratio agrees very well with the one produced by simulation.

We next examine the effect of unknown/unmodeled interference. In addition to the Capon receiver, we also consider another linear blind scheme implemented by first applying the MUSIC blind channel estimator [24] and then using the channel estimate in the MMSE receiver for detection. We first simulate a scenario involving ICI by letting K' ($K' \leq K$) out of $K = 10$ equipow-

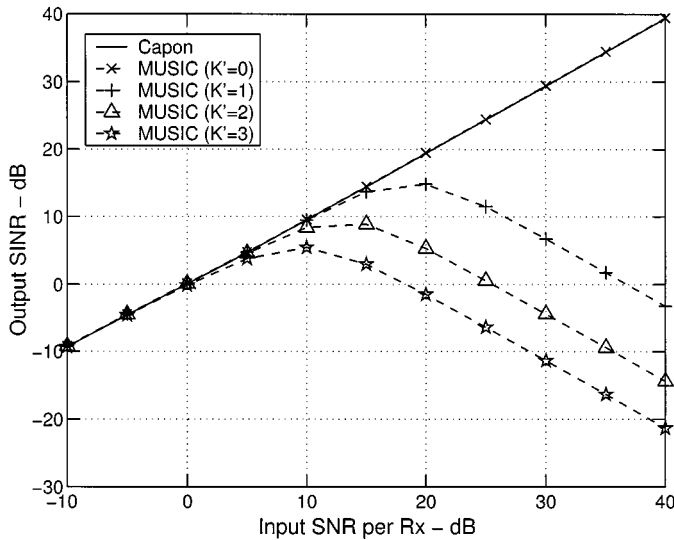


Fig. 2. Output SINR of the blind Capon and MUSIC receivers for $N = 2$ versus the input SNR per Rx when $J = 32$, $K = 10$, $NFR = 0$ dB and ICI is present (K' is the total number of ICI signals).

ered transmissions be originated from some neighboring cells. We assume that the MUSIC receiver, being ignorant of the ICI, is provided with the incorrect number of transmissions $K - K'$. We note that although model detection schemes can be used to estimate the number of transmissions [28], it is not unusual to misestimate the number of transmissions by a small number. Fig. 2 depicts the output SINR as a function of the input SNR per Rx when $N = 2$. Since the Capon receiver does not need the information of the number of transmissions, its performance remains unaffected as long as the level of the overall interference is unchanged. On the other hand, MUSIC yields a similar output SINR to that of Capon in the absence of ICI but degrades considerably when ICI is present.

The effect of narrowband interference is considered next. We simulate a scenario involving $K = 10$ equipowered user signals contaminated by a white Gaussian channel noise as well as a narrowband interference signal that is generated by a first-order autoregressive process [21] $i(t) = 0.99i(t-1) + e(t)$, where $e(t)$ is a white Gaussian process with zero-mean and variance σ_e^2 . The interference-to-signal ratio (ISR) for the desired (first) user as $ISR := (1/\rho_1) \int_{-1/2}^{1/2} \phi_i(f) df$, where $\phi_i(f)$ is the power spectral density of $i(t)$, and ρ_1 is the received signal power of the first user [see (1) and (2)]. Fig. 3 shows the output SINR versus the input SNR for both the Capon and MUSIC receiver with $N = 2$. We see that as the ISR increases (from -10 dB to 3 dB), the performance of Capon degrades gracefully, whereas the degradation of MUSIC is much more dramatic.

In the next example, we study the convergence property of the Capon receiver by replacing \mathbf{R}_{yy} with the sample estimate $\hat{\mathbf{R}}_{yy}$ in (24). We choose $SNR = 20$ dB and vary T [see (7)], whereas the other parameters are similar to those in the first example. Recall that when $\hat{\mathbf{R}}_{yy}$ is used in place of the true covariance matrix \mathbf{R}_{yy} , it is preferable to use (18) rather than (23) to compute $\mathbf{\Omega}$. Fig. 4(a) and (b) shows the channel estimation error and the output SINR, respectively, as a function of T . It is noted that the output SINR for $N = 2$ is smaller than that for $N = 1$ when T is small. This is because the Capon receiver has more degrees

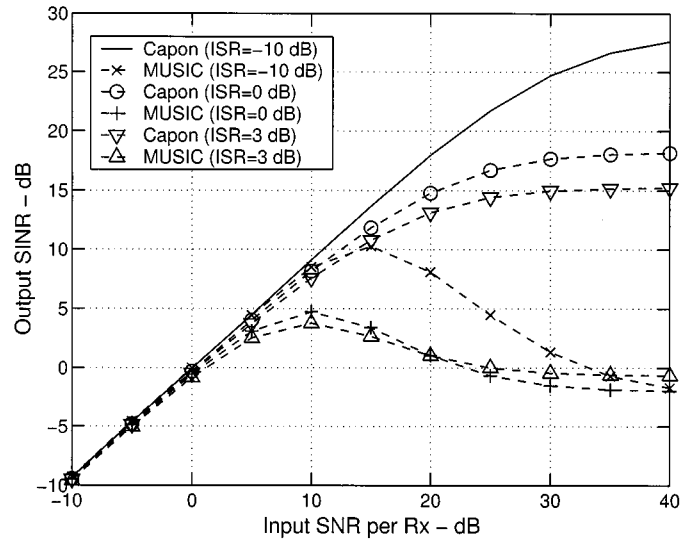
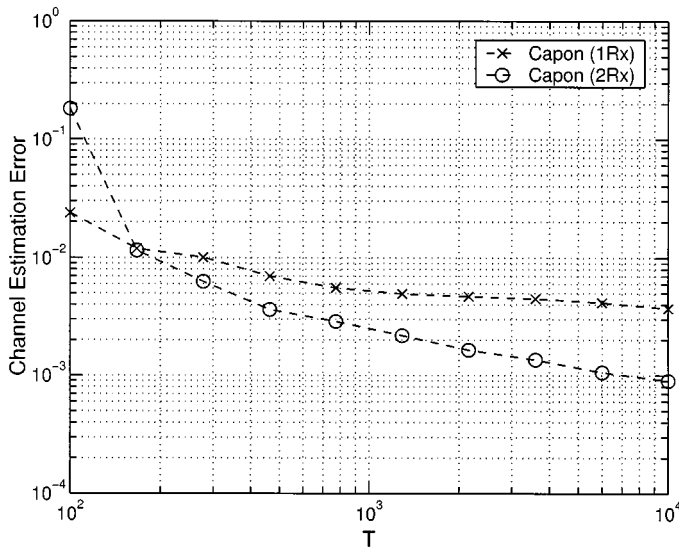


Fig. 3. Output SINR of the blind Capon and MUSIC receivers for $N = 2$ versus the input SNR per Rx when $J = 32$, $K = 10$, $NFR = 0$ dB, and narrowband interference is present.

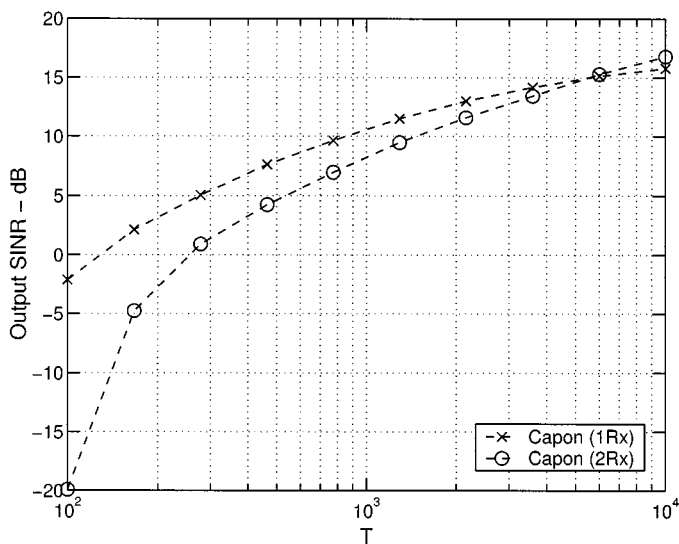
of freedom (i.e., $2NJ$ tap weights) when $N = 2$, which leads to a slower convergence rate.

Finally, we examine the semi-blind Capon receiver proposed in Section VI. We simulate a slowly time-varying fading scenario according to the Jakes' model [29] with a terminal speed of 3 m/s and a normalized Doppler rate of 1.6×10^{-5} . We consider the MMSE and Capon receivers with and without the CSI. When the CSI is not available, the MMSE receiver uses periodic training to derive an estimate of the CSI, with a training cycle of $T = 1000$ blocks and a 15% training overhead. The Capon without CSI is implemented by the semi-blind approach, which utilizes initial training for starting and pilots-assisted blind adaptation afterwards. The Capon channel estimate and receiver are updated every $T_C = 50$ blocks, using $T_P = 2$ blocks as pilots to resolve the scalar ambiguity. Hence, the overhead for the semi-blind Capon approach is 4% (excluding the initial training). The covariance matrix is computed recursively using a sliding window [cf. (37)–(39)] of length $W = 1000$ when $N = 1$ and $W = 2500$ when $N = 2$, respectively. The system consists of $K = 10$ users, with an NFR of 10 dB for the desired user. The bit-error rate (BER) for the various receivers presented below is averaged over 100 independent channels.

Fig. 5(a) depicts the BER as a function of the SNR per Rx. We note that the Capon and MMSE receivers with CSI (2Tx) attain almost identical BER. The semi-blind Capon (2Tx) is slightly worse, with a performance loss less than 1 dB (in SNR) compared with the former. The semi-blind Capon (2Tx) also considerably outperforms the training-based MMSE receiver (2Tx), which has an error floor caused by channel variation. To show the merit of ST coding, we also include in Fig. 5(a) the BER of the conventional Capon receiver without ST coding (1Tx) [13]–[15] implemented by a semi-blind approach that is similar to the one in Section VI. A comparison of the two semi-blind Capon receivers indicates a quite substantial diversity gain offered by ST coding. For example, when $BER = 3 \times 10^{-3}$, the semi-blind Capon (2Tx) attains a 9-dB diversity gain over the semi-blind Capon (1Tx).



(a)



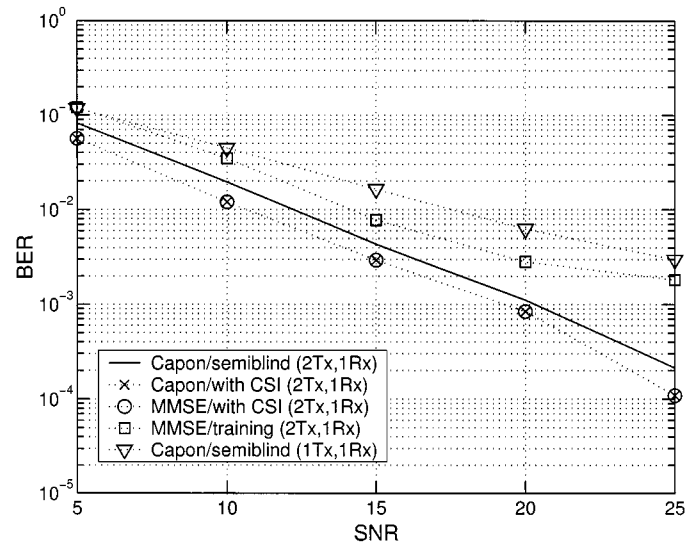
(b)

Fig. 4. Performance of the blind Capon receiver versus the number of code blocks T when $J = 32$, $K = 10$, $\text{SNR} = 20$ dB, and $\text{NFR} = 10$ dB. (a) Channel estimation error. (b) Output SINR.

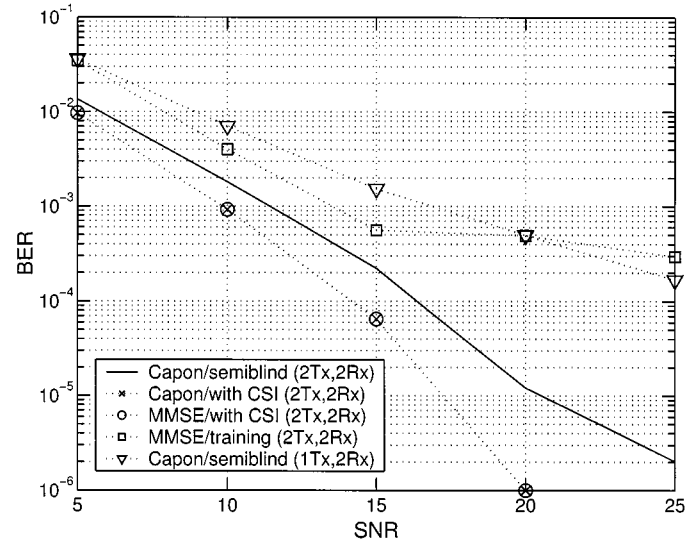
The BER of the various receivers equipped with $N = 2$ Rx's is shown Fig. 5(b). The training-based MMSE receiver (2Tx) is again worse than the semi-blind Capon receiver (2Tx), although the latter also suffers from a larger performance loss relative to the MMSE receiver with CSI (2Tx). The conventional semi-blind Capon receiver (1Tx) is also included to illustrate the diversity gain offered by ST coding.

VIII. CONCLUSION

We have studied the (semi-)blind Capon receiver for ST-block-coded CDMA systems. The Capon receiver requires only the spreading codes and timing for the desired user but little side information of the interfering signals. It does not model the interference/noise exactly and is capable of suppressing the overall interference signals. We have examined the ST coding-induced structure of the received signal and



(a)



(b)

Fig. 5. BER versus the input SNR per Rx in time-varying fading channels when $J = 32$, $K = 10$ and $\text{NFR} = 10$ dB. (a) $N = 1$. (b) $N = 2$.

established several analytical results based on this unique signal structure. We have shown that Capon receiver is by design immune to self interference. Both analytical and numerical results suggest that the Capon receiver achieves an output SINR similar to that of the linear optimum MMSE receiver and that the Capon channel estimate is SNR consistent. Numerical studies have also been presented to compare the blind Capon and MUSIC receivers in terms of the output SINR in the presence of unmodeled interference and to demonstrate the diversity gain of ST-coded CDMA systems over systems using no ST coding.

Our discussion has been focused on frequency-flat channels. Extension of the Capon receiver can be made to frequency-selective channels by combining ST coding and multicarrier CDMA systems, where the overall bandwidth is divided into a set of subchannels that are approximately frequency flat. Such extensions will be explored and reported in the future. Another interesting topic is related to the estimation of the covariance

matrix \mathbf{R}_{yy} . There may exist more data-efficient covariance matrix estimators that exploit the inherent signal structure imposed by ST coding. Such a structured covariance matrix estimator will speed up the convergence rate of not only the Capon receiver but of all other blind schemes that rely on an estimate of \mathbf{R}_{yy} as well.

APPENDIX A PROOF OF LEMMAS 1 AND 2

First, we prove Lemma 1. By direct calculation, it can be verified that

$$\bar{\mathbf{D}}_k = \mathbf{M}_{2J} \mathbf{D}_k. \quad (42)$$

Next, we note that $\bar{\mathbf{g}}_k = \bar{\mathbf{D}}_k \mathbf{h}^* = [\mathbf{I}_N \otimes (\mathbf{M}_{2J} \mathbf{D}_k)] \mathbf{h}^* = (\mathbf{I}_N \otimes \mathbf{M}_{2J}) \mathbf{D}_k \mathbf{h}^* = (\mathbf{I}_N \otimes \mathbf{M}_{2J}) \mathbf{g}_k^*$. Multiplying both sides of the above equation by $(\mathbf{I}_N \otimes \mathbf{M}_{2J})^{-1}$ while observing that $\mathbf{I}_N \otimes \mathbf{M}_{2J}$ is orthonormal (since \mathbf{M}_{2J} is so) yields (20). Equation (21) follows from (20) since $\mathbf{I}_N \otimes \mathbf{M}_{2J}$ is skew-symmetric, i.e., $(\mathbf{I}_N \otimes \mathbf{M}_{2J})^T = -(\mathbf{I}_N \otimes \mathbf{M}_{2J})$. ■

To prove Lemma 2, we note that

$$\begin{aligned} & (\mathbf{I}_N \otimes \mathbf{M}_{2J})^H \mathbf{R}_{yy} (\mathbf{I}_N \otimes \mathbf{M}_{2J}) \\ &= \sum_{k=1}^K \rho_k [(\mathbf{I}_N \otimes \mathbf{M}_{2J})^H \mathbf{g}_k \mathbf{g}_k^H (\mathbf{I}_N \otimes \mathbf{M}_{2J}) \\ &\quad + (\mathbf{I}_N \otimes \mathbf{M}_{2J})^H \bar{\mathbf{g}}_k \bar{\mathbf{g}}_k^H (\mathbf{I}_N \otimes \mathbf{M}_{2J})] + \sigma_w^2 \mathbf{I}_{2JN} \\ &= \sum_{k=1}^K \rho_k [(-\bar{\mathbf{g}}_k^*)(-\bar{\mathbf{g}}_k^*)^H + (\mathbf{g}_k^*)(\mathbf{g}_k^*)^H] + \sigma_w^2 \mathbf{I}_{2JN} = \mathbf{R}_{yy}^* \end{aligned}$$

where in the second equality, we used (20) and (21) (by replacing the generic \mathbf{g}_k and $\bar{\mathbf{g}}_k$ with the true \mathbf{g}_k and $\bar{\mathbf{g}}_k$, respectively). Taking the matrix inverse on both sides and, again, using the fact that $\mathbf{I}_N \otimes \mathbf{M}_{2J}$ is orthonormal, we arrive at (22). ■

APPENDIX B PROOF OF THEOREM 3

We first establish the existence of a perfect solution under the stated conditions. The limiting form of \mathbf{R}_{yy}^{-1} when the SNR goes to infinity is given by (e.g., [15]) $\lim_{\sigma_w^2 \rightarrow 0} \sigma_w^2 \mathbf{R}_{yy}^{-1} = \mathbf{E}_n \mathbf{E}_n^H$, where \mathbf{E}_n contains the noise eigenvectors of \mathbf{R}_{yy} [see (34)]. The observation, along with (18) and (23), suggests that

$$\lim_{\sigma_w^2 \rightarrow 0} \mathbf{h}_C(\sigma_w^2) = \arg \min_{\mathbf{h} \in \mathbb{C}^{2N \times 1}} \mathbf{h}^H [\mathbf{D}_1^H \mathbf{E}_n \mathbf{E}_n^H \mathbf{D}_1] \mathbf{h} \quad (43)$$

where, henceforth, we use \mathbf{h} as a dummy variable, whereas we use \mathbf{h} for the *true* channel. Note that $\mathbf{h}/\|\mathbf{h}\|$ minimizes the above criterion since $\mathbf{D}_1 \mathbf{h}/\|\mathbf{h}\| \in \text{ran}(\mathbf{E}_s)$, and therefore, the above criterion evaluated at $\mathbf{h}/\|\mathbf{h}\|$ is minimized (equal to zero). The uniqueness of this solution remains to be verified.

Let $\tilde{\mathbf{G}}_n := [\tilde{\mathbf{g}}_{1n}, \tilde{\mathbf{g}}_{2n}, \tilde{\mathbf{g}}_{2n}, \dots, \tilde{\mathbf{g}}_{Kn}, \tilde{\mathbf{g}}_{Kn}]$ and $\tilde{\mathbf{G}} := [\tilde{\mathbf{G}}_1^T, \dots, \tilde{\mathbf{G}}_N^T]^T$. Before we go on to prove the uniqueness of $\mathbf{h}/\|\mathbf{h}\|$, we show that the conditions stated in Theorem 3 imply the columns of $\mathbf{D}_1 \notin \text{ran}(\tilde{\mathbf{G}}_n)$ at least for one n . This is seen by contradiction. Note that the first and second columns of \mathbf{D}_1 are given by $[\mathbf{c}_{11}^T, \mathbf{0}^T]^T$ and $[\mathbf{0}^T, \mathbf{c}_{21}^T]^T$, respectively [cf. (5)]. Assume without loss of

generality that $\mathbf{h}_n = [h_{1n}, h_{2n}^*]^T \neq \mathbf{0}$ and that there exist nontrivial $\boldsymbol{\beta} = [\beta_{21}, \beta_{12}, \beta_{22}, \dots, \beta_{1K}, \beta_{2K}]^T \in \mathbb{C}^{(2K-1) \times 1}$ and $\boldsymbol{\gamma} = [\gamma_{21}, \gamma_{12}, \gamma_{22}, \dots, \gamma_{1K}, \gamma_{2K}]^T \in \mathbb{C}^{(2K-1) \times 1}$ such that $[\mathbf{c}_{11}^T, \mathbf{0}^T]^T = \tilde{\mathbf{G}}_n \boldsymbol{\beta}$ and $[\mathbf{0}^T, \mathbf{c}_{21}^T]^T = \tilde{\mathbf{G}}_n \boldsymbol{\gamma}$. Substituting (3) and (4) into the above expressions yields

$$\begin{aligned} \mathbf{c}_{11} &= \beta_{21} h_{2n} \mathbf{c}_{21} + \sum_{k=2}^K (\beta_{1k} h_{1n} \mathbf{c}_{1k} + \beta_{2k} h_{2n} \mathbf{c}_{2k}) \\ \mathbf{c}_{21} &= -\gamma_{21} h_{1n}^* \mathbf{c}_{11} + \sum_{k=2}^K (\gamma_{1k} h_{2n}^* \mathbf{c}_{2k} - \gamma_{2k} h_{1n}^* \mathbf{c}_{1k}) \end{aligned}$$

which contradict the conditions stated in Theorem 3. Hence, the columns of $\mathbf{D}_1 \notin \text{ran}(\tilde{\mathbf{G}}_n)$.

The proof of uniqueness proceeds again by contradiction. Assume there exists \mathbf{h}' linearly independent of $\mathbf{h}/\|\mathbf{h}\|$ and $\mathbf{g}'_1 = \mathbf{D}_1 \mathbf{h}' \in \text{ran}(\mathbf{E}_s)$, which also minimizes the criterion (43). We note that $\mathbf{g}'_1 \in \text{ran}(\mathbf{G})$ since $\text{ran}(\mathbf{E}_s) = \text{ran}(\mathbf{G})$, where $\mathbf{G} = [\mathbf{g}_1, \tilde{\mathbf{G}}]$. It follows that there exist nontrivial $\boldsymbol{\theta} \in \mathbb{C}^{(2K-1) \times 1}$ and $\phi \in \mathbb{C}^{1 \times 1}$ such that $\mathbf{D}_1 \mathbf{h}' = \tilde{\mathbf{G}} \boldsymbol{\theta} + \phi \mathbf{g}_1$ or, equivalently

$$\mathbf{D}_1 (\mathbf{h}' - \phi \mathbf{h}) = \tilde{\mathbf{G}} \boldsymbol{\theta}. \quad (44)$$

Let $\Delta \mathbf{h} := \mathbf{h}' - \phi \mathbf{h} := [\Delta \mathbf{h}_1, \dots, \Delta \mathbf{h}_N]$, and note that $\{\Delta \mathbf{h}_n\}_{n=1}^N$ are not identically equal to zero. Then, (44) is equivalent to

$$\mathbf{D}_1 \Delta \mathbf{h}_n = \tilde{\mathbf{G}}_n \boldsymbol{\theta}, \quad n = 1, \dots, N$$

which contradicts the previously established fact that the columns of $\mathbf{D}_1 \notin \text{ran}(\tilde{\mathbf{G}}_n)$ for at least one n . Hence, $\mathbf{h}/\|\mathbf{h}\|$ is the unique solution to (43). ■

REFERENCES

- [1] (1998, Nov.) Tetherless T3 and Beyond. NSF. [Online]. Available: <http://www.cudenver.edu/public/engineer/T3-Workshop/T3Report-12-98.htm>
- [2] A. F. Naguib, N. Seshadri, and A. R. Calderbank, "Increasing data rate over wireless channels," *IEEE Signal Processing Mag.*, vol. 17, pp. 76–92, May 2000.
- [3] Z. Liu, G. B. Giannakis, B. Muquet, and S. Zhou, "Space-time coding for broadband wireless communications," *Wireless Syst. Mobile Comput.*, vol. 1, no. 1, pp. 35–53, Jan.–Mar. 2001.
- [4] V. Tarokh, N. Seshadri, and A. R. Calderbank, "Space-time codes for high data rate wireless communications: Performance criterion and code construction," *IEEE Trans. Inform. Theory*, vol. 44, pp. 744–765, Mar. 1998.
- [5] S. M. Alamouti, "A simple transmit diversity techniques for wireless communications," *IEEE J. Select. Areas Commun.*, vol. 16, pp. 1451–1458, Oct. 1998.
- [6] V. Tarokh, H. Jafarkhani, and A. R. Calderbank, "Space-time block codes from orthogonal designs," *IEEE Trans. Inform. Theory*, vol. 45, pp. 1456–1467, July 1999.
- [7] B. L. Hughes, "Differential space-time modulation," *IEEE Trans. Inform. Theory*, vol. 46, pp. 2567–2578, Nov. 2000.
- [8] B. M. Hochwald and W. Sweldens, "Differential unitary space-time modulation," *IEEE Trans. Commun.*, vol. 48, pp. 2041–2052, Dec. 2000.
- [9] V. Tarokh and H. Jafarkhani, "A differential detection scheme for transmit diversity," *IEEE J. Select. Areas Commun.*, vol. 18, pp. 1169–1174, July 2000.
- [10] Z. Liu, G. B. Giannakis, and B. L. Hughes, "Double differential space-time block coding for time-varying fading channels," *IEEE Trans. Commun.*, vol. 49, pp. 1529–1539, Sept. 2001.
- [11] J. Liu, J. Li, H. Li, and E. G. Larsson, "Differential space-code modulation for interference suppression," *IEEE Trans. Signal Processing*, vol. 49, pp. 1786–1795, Aug. 2001.

- [12] J. Capon, "High resolution frequency-wavenumber spectrum analysis," *Proc. IEEE*, vol. 57, no. 8, pp. 1408–1418, Aug. 1969.
- [13] M. L. Honig, U. Madhow, and S. Verdú, "Blind adaptive multiuser detection," *IEEE Trans. Inform. Theory*, vol. 41, pp. 944–960, July 1995.
- [14] J. B. Schodorf and D. B. Williams, "A constrained optimization approach to multiuser detection," *IEEE Trans. Signal Processing*, vol. 45, pp. 258–262, Jan. 1997.
- [15] M. K. Tsatsanis and Z. Xu, "Performance analysis of minimum variance CDMA receiver," *IEEE Trans. Signal Processing*, vol. 46, pp. 3014–3022, Nov. 1998.
- [16] P. Bender, P. Black, M. Grob, R. Padovani, N. Sindhushayana, and A. Viterbi, "CDMA/HDR: A bandwidth-efficient high-speed wireless data service for nomadic users," *IEEE Commun. Mag.*, vol. 38, no. 7, pp. 70–77, July 2000.
- [17] G. H. Golub and C. F. Van Loan, *Matrix Computations*, 3rd ed. Baltimore, MD: Johns Hopkins Univ. Press, 1996.
- [18] *Space-Time Block Coded Transmit Antenna Diversity for WCDMA*, Dec. 1998. proposed TDOC#662/98 to ETSI SMG2 UMTS Stand. .
- [19] B. Hochwald, T. L. Marzetta, and C. B. Papadias, "A transmitter diversity scheme for wideband CDMA systems based on space-time spreading," *IEEE J. Select. Areas Commun.*, vol. 19, pp. 48–60, Jan. 2001.
- [20] *Downlink Improvement Through Space-Time Spreading*, Aug. 1999. Lucent Technol. proposal 3GPP2-C30-19 990 817-014 to the IS-2000 Stand..
- [21] H. V. Poor, "Active interference suppression in CDMA overlay systems," *IEEE J. Select. Areas Commun.*, vol. 19, pp. 4–20, Jan. 2001.
- [22] S. Haykin, *Adaptive Filter Theory*, 3rd ed. Upper Saddle River, NJ: Prentice-Hall, 1996.
- [23] O. L. Frost III, "An algorithm for linearly constrained adaptive array processing," *Proc. IEEE*, vol. 60, pp. 926–935, Aug. 1972.
- [24] E. Moulines, P. Duhamel, J.-F. Cardoso, and S. Mayrargue, "Subspace methods for the blind identification of multichannel FIR filters," *IEEE Trans. Signal Processing*, vol. 43, pp. 516–525, Feb. 1995.
- [25] H. Li, J. Li, and P. Stoica, "Performance analysis of forward-backward matched-filterbank spectral estimators," *IEEE Trans. Signal Processing*, vol. 46, pp. 1954–1966, July 1998.
- [26] P. Stoica, H. Li, and J. Li, "Amplitude estimation of sinusoidal signals: Survey, new results, and an application," *IEEE Trans. Signal Processing*, vol. 48, pp. 338–352, Feb. 2000.
- [27] L. Tong and S. Perreau, "Multichannel blind identification: From subspace to maximum likelihood methods," *Proc. IEEE*, vol. 86, pp. 1951–1968, Oct. 1998.
- [28] M. Wax and T. Kailath, "Detection of signals by information theoretic criteria," *IEEE Trans. Acoust., Speech Signal Processing*, vol. ASSP-33, pp. 387–392, Apr. 1985.
- [29] W. C. Jakes Jr., *Microwave Mobile Communications*. New York: Wiley-Interscience, 1974.



Hongbin Li (M'99) received the B.S. and M.S. degrees from the University of Electronic Science and Technology of China (UESTC) in 1991 and 1994, respectively, and the Ph.D. degree from the University of Florida, Gainesville, in 1999, all in electrical engineering.

From July 1996 to May 1999, he was a Research Assistant with the Department of Electrical and Computer Engineering, University of Florida. Since July 1999, he has been an Assistant Professor with the Department of Electrical and Computer Engineering,

Stevens Institute of Technology, Hoboken, NJ. His current research interests include stochastic signal processing, sensor array processing, wireless communications, and radar imaging.

Dr. Li is a member of Tau Beta Pi and Phi Kappa Phi. He received the Jess H. Davis Memorial Award for excellence in research from Stevens Institute of Technology in 2001 and the Sigma Xi Graduate Research Award from the University of Florida in 1999.



Xuguang Lu received the B.E. and M.E. degrees from the University of Science and Technology of China (USTC) in 1989 and 1992, respectively, and the Ph.D. degree from Stevens Institute of Technology, Hoboken, NJ, in 2001, all in electrical engineering.

From 1992 to 1997, he was with China Telecom, Shenzhen. He is currently a Member of Technical Staff with Bell Laboratories, Lucent Technologies. His major research interest is third-generation wireless communications.



Georgios B. Giannakis (F'97) received the Diploma in electrical engineering from the National Technical University of Athens, Athens, Greece in 1981. He received the M.Sc. degree in electrical engineering in 1983, the M.Sc. degree in mathematics in 1986, and the Ph.D. degree in electrical engineering in 1986, all from the University of Southern California (USC), Los Angeles.

After lecturing for one year at USC, he joined the University of Virginia, Charlottesville, in 1987, where he became a Professor of Electrical Engineering in 1997. Since 1999 he has been a Professor with the Department of Electrical and Computer Engineering, University of Minnesota, Minneapolis, where he now holds an ADC Chair in Wireless Telecommunications. His general interests span the areas of communications and signal processing, estimation and detection theory, time-series analysis, and system identification—subjects on which he has published more than 140 journal papers, 270 conference papers, and two edited books. Current research topics focus on transmitter and receiver diversity techniques for single- and multiuser fading communication channels, precoding and space-time coding for block transmissions, and multicarrier and wideband wireless communication systems.

Dr. Giannakis is the (co-) recipient of three best paper awards from the IEEE Signal Processing (SP) Society (in 1992, 1998, and 2000). He also received the Society's Technical Achievement Award in 2000. He co-organized three IEEE-SP Workshops and guest (co-) edited four special issues. He has served as Editor in Chief for the IEEE SIGNAL PROCESSING LETTERS, as Associate Editor for the IEEE TRANSACTIONS ON SIGNAL PROCESSING and the IEEE SIGNAL PROCESSING LETTERS, as Secretary of the SP Conference Board, as Member of the SP Publications Board, as Member and Vice-Chair of the Statistical Signal and Array Processing Technical Committee, and as Chair of the SP for Communications Technical Committee. He is a member of the Editorial Board for the PROCEEDINGS OF THE IEEE, and the steering committee of the IEEE TRANSACTIONS ON WIRELESS COMMUNICATIONS. He is a member of the IEEE Fellows Election Committee, the IEEE-SP Society's Board of Governors, and a frequent consultant for the telecommunications industry.